Energy Technology
Generation, Conversion, Storage, Distribution

RESEARCH ARTICLE

Upcycling Expired Silicone Sealants into High-Performance Triboelectric Nanogenerators for Sustainable Energy Harvesting and Smart Infrastructure Safety Systems

Anusha Kaki[1] | Mahesh Velpula[1] | Navaneeth Madathil[1] | Khanapuram Uday Kumar[1] | Ravinder Reddy Kisannagar[2] | Inhwa Jung[2] | Rakesh Kumar Rajaboina[1]

[1]Department of Physics, Energy Materials and Devices (EMD) Lab, National Institute of Technology, Warangal, India | [2]Department of Mechanical Engineering, Kyung Hee University, Yongin, Republic of Korea

Correspondence: Rakesh Kumar Rajaboina (rakeshr@nitw.ac.in)

Received: 25 September 2025 | **Revised:** 20 November 2025 | **Accepted:** 22 December 2025

Keywords: energy harvesting | industrial waste | self-powered electronics | silicone sealant | triboelectric nanogenerators | waste to energy

ABSTRACT

The present study addresses the industrial waste management of nonbiodegradable expired/waste silicone sealants (SS) through triboelectric nanogenerator technology (TENG). It explores the upcycling of waste SS as a frictional layer in a TENG to harness mechanical energy for sustainable applications. Among all the fabricated TENG devices, the SS-fluorinated ethylene propylene (FEP) frictional pair generated a maximum V_{oc} of ~320 V and I_{sc} of ~145 μA, with an instantaneous power density of 5.7 W/m^2. The device demonstrated excellent stability over 4000 cycles, allowing reliable operation in powering 240 light emitting diodes (LEDs), four LED lamps, and portable electronic devices such as calculators and digital watches through a charged capacitor. Finally, the SS-FEP TENG was utilized in a rail switch sensor system to monitor switch movements and provide real-time track status for enhanced rail safety.

1 | Introduction

Environmental protection has become a critical global concern due to the increasing pollution of air, water, and soil, largely driven by rapid technological advancements, irresponsible consumption patterns, and inadequate waste management practices [1, 2]. Addressing these challenges requires a strong commitment to the United Nations Sustainable Development Goals (SDGs: 12,7), which aim to safeguard the environment and promote a sustainable and green future for coming generations [3, 4]. Among the major contributors to environmental degradation is the growing volume of waste generated across various sectors, highlighting the urgent need for innovative and efficient waste management strategies. The waste management strategies include reuse, recycling, upcycling, waste-to-energy (WTE) technologies, composting, landfill management, policy, and public awareness [5]. Among all, WTE technologies stand out as a promising solution [6–11]. With WTE technologies, waste materials will be utilized to produce gas, oil, or electricity, and the amount of waste materials that are sent to landfills will be considerably reduced. WTE technologies are essential in protecting the environment and people's health. In recent years, triboelectric nanogenerator (TENG) technology has emerged as a novel addition to WTE approaches by effectively utilizing a wide range of waste materials for energy harvesting [12–15]. In previous studies, researchers have explored waste materials, including plastic [16–19], medical [20–23], construction [24], electronic [25–30], and bio-waste [31–35], to fabricate TENGs and employ them for energy harvesting and sensing applications [36–41].

Silicone sealant (SS) is a versatile material widely used across various industries due to its flexibility, waterproofing ability, and chemical resistance. SS has a limited shelf life of approximately 12–24 months, often resulting in expired or partially used cartridges and tubes being discarded as waste. If the expired SS

remains pliable, it can effectively be used to create a frictional layer on a conductive substrate for TENG applications. However, care must be taken; if the sealant is partially cured, it becomes difficult to form a uniform frictional layer. The triboelectric properties of SS are influenced by the fillers, chemical process involved in the manufacturing, which also modify the sealant's appearance. Various types of sealants, including clear, black, white, and red, can be formulated with fillers such as silica, carbon black, titanium dioxide, and iron oxide [42].

In this work, black SS waste is utilized as a triboelectric layer in TENG fabrication for energy harvesting and rail switch sensor applications. Compared with other waste materials, such as rigid plastic scraps, multilayer medical blister packs, or mechanically fragile packaging films used in TENG, expired SS offers several advantages. The advantages included excellent mechanical flexibility and strong inherent adhesion to metallic substrates, enabling it to be directly coated onto aluminum surfaces with robust interfacial contact. This eliminates the need for separate electrode attachment or adhesive layers, which are often required when using conventional waste plastics. Additionally, unlike many waste-derived materials that require high-temperature melting, solvent-based dissolution, or multistep lamination, SS can be processed at room temperature, cures without solvents, and remains highly cost-effective. These advantages collectively make expired SS a more practical, scalable, and application-ready waste material for TENG fabrication. The fabricated TENG exhibited a peak output of ~320 V and 145 μA, with a power density of 5.7 W/m^2 and stable performance over 4000 cycles. It successfully powered a series of LEDs, multiple LED lamps, and portable electronic devices such as calculators and digital watches using a storage element.

2 | Experimental

2.1 | TENG Device Fabrication

An expired black SS tube was collected from household waste, where the material remained pliable. A photograph of the collected SS tube is shown in Figure 1a. The SS was film-cast onto a predesigned glass mold containing a $5 \times 5\ cm^2$ aluminum substrate placed at the bottom. After curing under ambient conditions, a fully adhesive black SS film was formed on the aluminum surface and used as one of the triboelectric layers for TENG fabrication. The TENG was fabricated by attaching the SS-coated aluminum substrate to a predesigned cardboard sheet, as shown in Figure 1b. Another cardboard sheet was prepared with the opposite triboelectric material, and the corresponding frictional layer was attached to an aluminum sheet using conductive tape. Figure 1b displays the photographs of the assembled TENG device operating in vertical contact–separation mode,

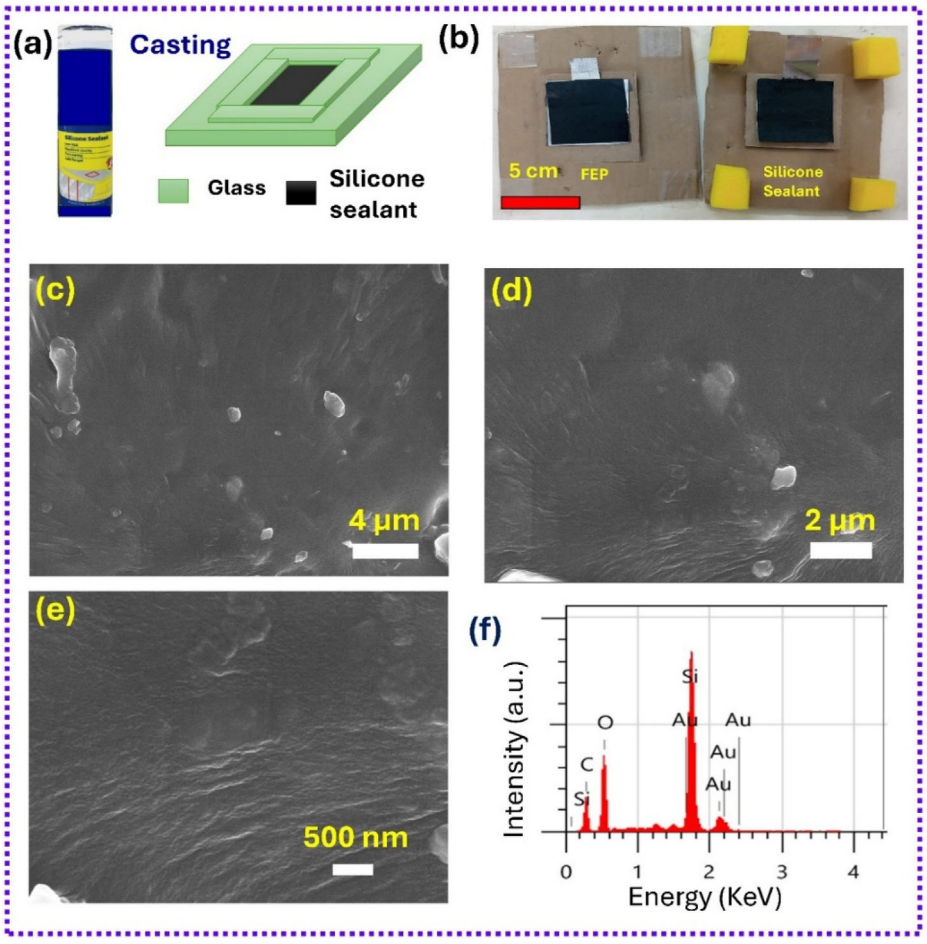

FIGURE 1 | (a) Photograph of the SS tube and casting of film on glass mold, (b) fabricated TENG device with FEP and SS frictional layers, (c–e) surface texture of the coated SS film on aluminum at different magnifications, (f) EDX spectrum of the coated SS film. EDX= energy-dispersive X-ray spectrum; FEP = fluorinated ethylene propylene; SS = silicone sealant; TENG = triboelectric nanogenerator technology.

with SS and FEP serving as the frictional layers. This device was referred to as the SS-FEP TENG. A total of eight TENG devices were fabricated, each incorporating a different counter triboelectric material. The spacing between the frictional layers was maintained using sponge spacers, allowing a separation distance of approximately 1 cm.

2.2 | Structural and Electrical Characterization

The morphology of the SS was examined using scanning electron microscopy (SEM, *JEOL JSM IT-800.*). The electrical output of the TENGs was measured using a digital storage oscilloscope (GW-Instek, GDS-1102B) and a current preamplifier (SRS, SR-570). The surface potential of the triboelectric layers was measured using a Trek 542A electrostatic voltmeter. The TENG was tested under hand tapping force at a frequency of 4–5 Hz at room temperature. The load characteristics of TENG were assessed with a decade resistance box. The rail switch sensor application was performed with Arduino board (UNO R3).

3 | Results and Discussion

The surface texture of the coated SS film at different magnifications was recorded with SEM, and images are presented in Figure 1c–e. The SEM images reveal a continuous, irregularly textured coating. The irregularly textured coating results in a relatively rough texture, which may enhance surface area and could influence triboelectric performance in device applications. Figure 1f shows the energy-dispersive X-ray spectrum (EDX) of the coated SS film. The EDX confirms that the coated layer is composed of silicon and oxygen, consistent with the silicone polymer matrix. The presence of gold (Au) peaks in the spectrum is due to the gold coating applied to the SS layer to prevent charging and enable proper image recording.

The mechanical energy harvesting capability of the TENGs was studied under hand-tapping force at a frequency of 4–5 Hz at room temperature. Figure 2a,b displays the open circuit voltage (V_{oc}) and short circuit current (I_{sc}) responses of the TENGs with the fixed SS layer paired with various opposing triboelectric layers. It is worth noting that TENG produced a relatively higher output voltage with tribo-negative frictional layers (silicone rubber, FEP, and PTFE) and a lower output voltage with tribo-positive materials (Al, Cu, and Kapton). Further, SS produced the highest voltage and current when FEP was used as the opposite frictional layer.

This observation contradicts the expected trend, as silicone is a well-known triboelectrically negative material, and when paired with another triboelectrically negative material (FEP), a lower output voltage is typically expected [43]. The change in the polarity of the SS might be due to the addition of additional additives or chemical modifications done during the manufacturing process. Furthermore, to verify the tribopolarity of the silicone waste material, we conducted two additional sets of experiments. First, we measured the surface potential of the silicone waste film after contact with different frictional layers (FEP, silicone rubber, Kapton, and PET). The corresponding surface potential plots are shown in Figure 2c. The results clearly demonstrate that the silicone waste develops a positive surface potential after contact with FEP and silicone rubber, whereas it becomes negatively charged after contact with Kapton and PET. This confirms the positive triboelectric nature of the silicone waste film when

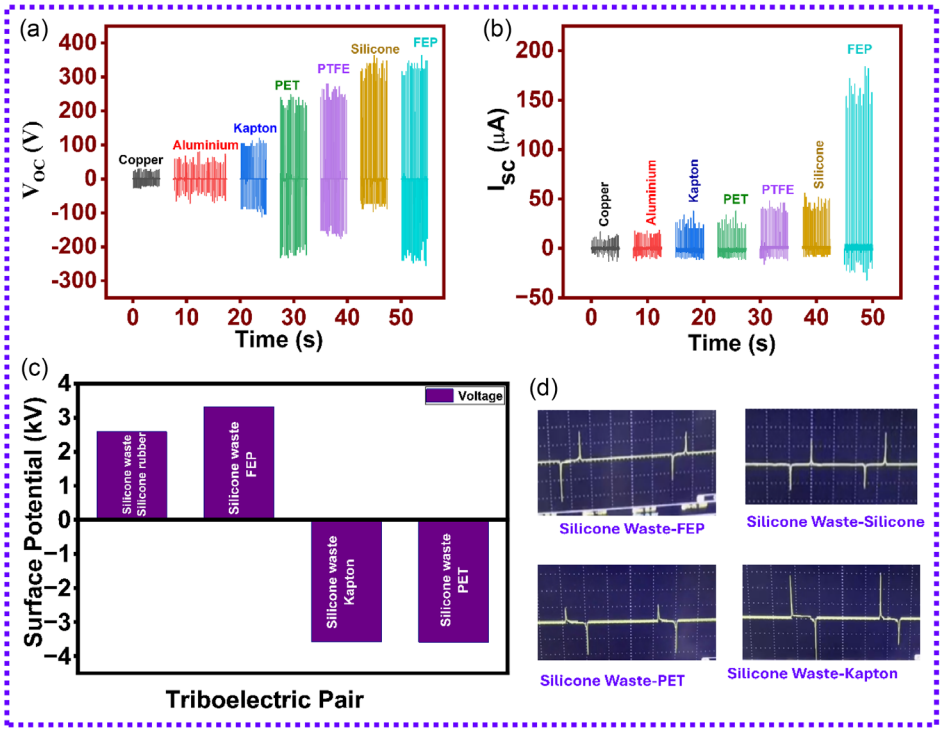

FIGURE 2 | (a,b) V_{oc} and I_{sc} of fabricated expired SS-based TENG with different opposite frictional layers, (c) surface potential values of SS film after contacting with different frictional layers, (d) output voltage polarity of different triboelectric pairs. SS = silicone sealants; TENG = triboelectric nanogenerator technology.

paired with strongly electronegative materials. A real-time demonstration of these surface potential variations with FEP and Kapton is provided in the Video S1, supporting information. In the second part, we recorded the output voltage signals of TENG devices fabricated using the silicone waste film paired with different frictional layers. A clear polarity reversal of the output voltage was observed when switching from silicone waste–FEP/silicone pairs to silicone waste–Kapton/PET pairs, as shown in Figure 2d and Video S2, supporting information. This further supports that the silicone waste behaves as a tribo-positive material with FEP/silicone and tribo-negative with Kapton/PET.

Additionally, we confirmed this trend using expired commercial transparent SS films. This film also consistently showed similar tribo-positive characteristics, verifying that the observed behavior is inherent to the SS waste material. The TENG responses of transparent silicone waste-based TENG are presented in Figure S1. From the above experimental observations, it is clear that the SS acts as a positive triboelectric layer. The maximum output performance ($V_{oc} \sim 320$ V, $I_{sc} \sim 145$ μA) was observed for the SS-FEP TENG, which was then used for further characterization.

Figure 3a,b shows the switching polarity test results of the SS-FEP TENG, clearly confirming that the electrical output is generated solely from the TENG devices and not from noise or other artifacts. The electrical output of TENG changes its sign upon switching the connections, while the noise does not change its sign. The SS-FEP TENG load characteristics were studied using a decade resistance box in the range of 1 KΩ to 100 MΩ. The output voltage and current values at different load resistances are presented in Figure 3c. The load characteristics trend of SS-FEP TENG is consistent with the reported literature [44]. The instantaneous power density $\left(P = \frac{V^2}{(R_L * A)}\right)$ was measured using the load characteristics data and the active area of the frictional layers and is presented in Figure 3d. The power density initially increased with load resistance, reaching a maximum of 5.7 W/m^2 at 1 MΩ, then decreased. The load resistance at which the maximum power density is achieved is considered the load matching condition, as per the maximum power transfer theorem [45]. Long-term stability is crucial to ensuring their reliability and practical applicability in sustainable energy-harvesting and sensing applications. The stability of the TENG was evaluated over 4000 test cycles, and it was found that the TENG electrical output was consistent, as shown in Figure 3e.

Initially, the TENG output was rectified using a bridge rectifier and powered 240 LEDs, four LED lamps momentarily for each hand tap, as shown in Figure 4a–c. The corresponding real-time demonstrations are provided in Videos S3 and S4, supporting information. Furthermore, a few portable electronic devices were powered by TENG using a charged capacitor; the circuit schematic is shown in Figure 4d. Initially, TENG output was rectified using a DB 107 full-wave rectifier and then used as input to the capacitor for charging. After the capacitor reached a sufficient charge level, devices (such as calculators and digital watches) were connected to power them for short periods. In the case of the calculator, the capacitor was charged to 1.6 V in 48 s and then powered the calculator for 14 s (Video S5, supporting information). During that time, mathematical calculations were performed. In the case of a digital watch, the capacitor was charged to 1.5 V in 48 s and then powered the digital watch for 16 s (Video S6, supporting information). Further, these devices can be made into fully self-powered ones if a continuous mechanical motion is attached to them.

Figure 5a shows the experimental design setup prepared from rigid cardboard sheets, representing a railway switch with main and diverging tracks highlighted in red and blue color. The rail switch is a mechanical device installed on railway tracks that allows trains to transition from one track to another, such as at junctions, sidings, or points where tracks diverge or converge. It also enables the track signals (red/green) on the track to inform

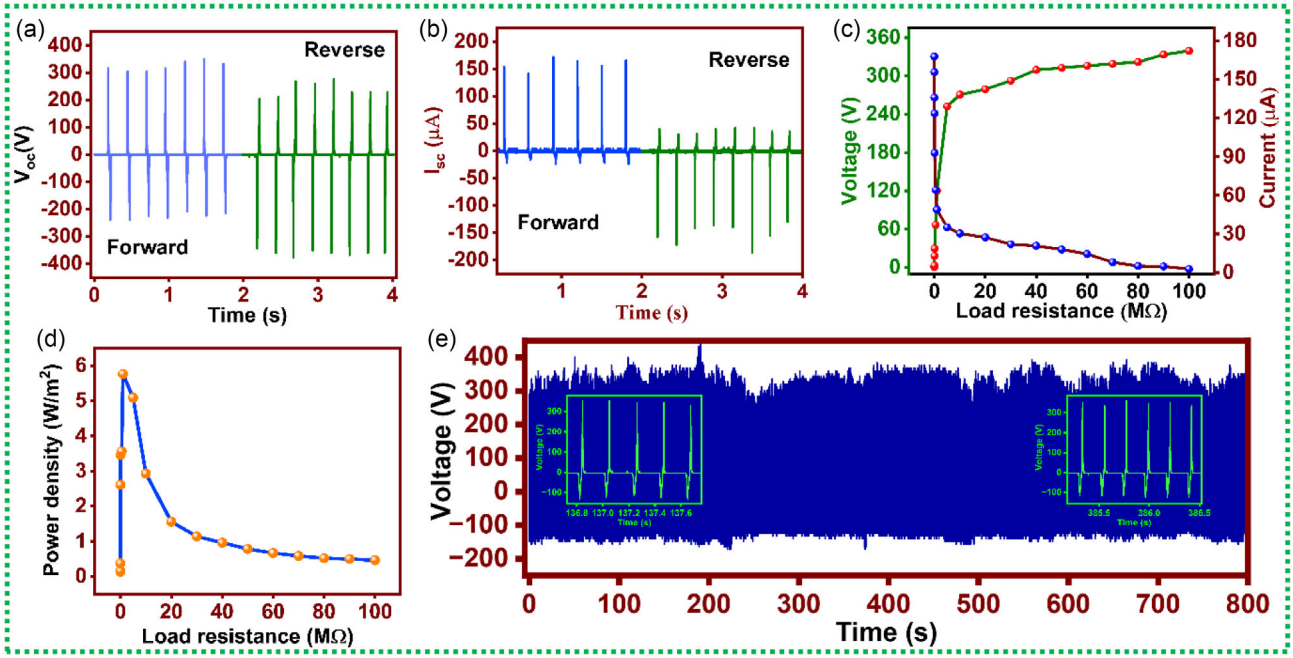

FIGURE 3 | (a,b) SS-FEP TENG switching polarity test output, (c) load characteristics, (d) power density at different loads, (e) stability of the TENG over 4000 cycles (inset magnified view of a few cycles). TENG = triboelectric nanogenerator technology.

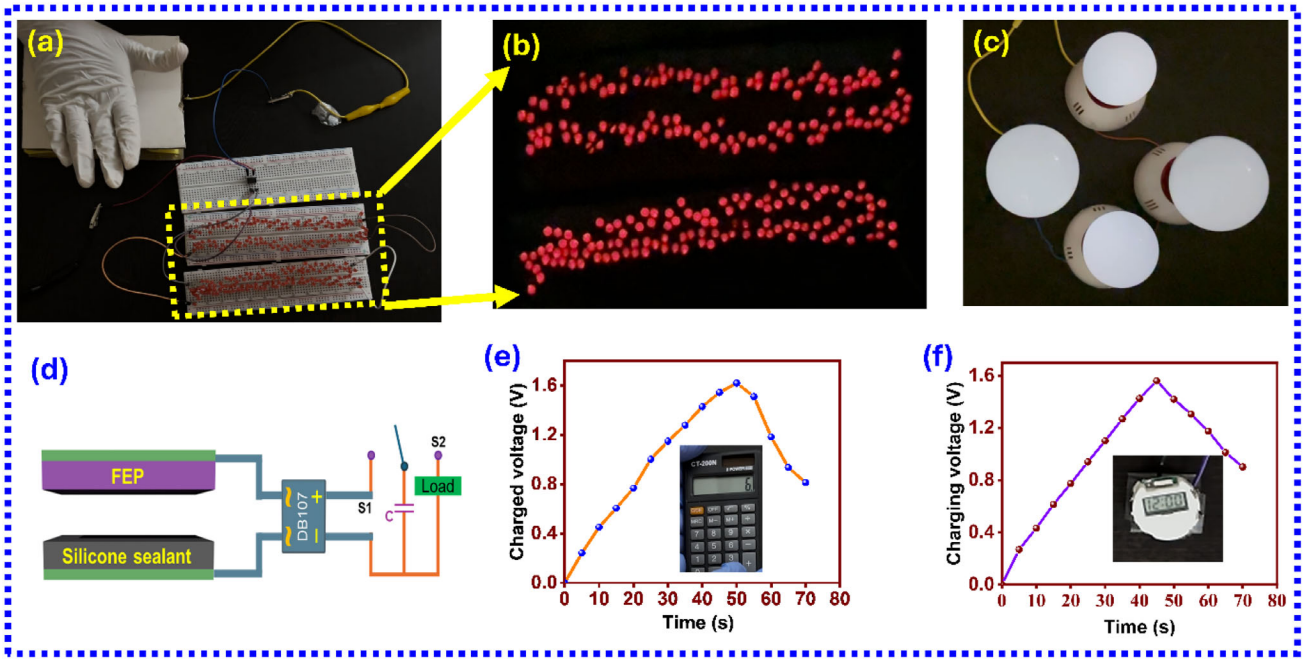

FIGURE 4 | (a) SS-FEP TENG connected to series-connected LEDs, powering, (b) 240 LEDs, (c) four LED lamps, (d) SS-FEP TENG with energy storage unit and two-way switch, (e,f) charging and discharging profiles of a capacitor while powering the electronic devices (inset photograph of the devices in ON condition).

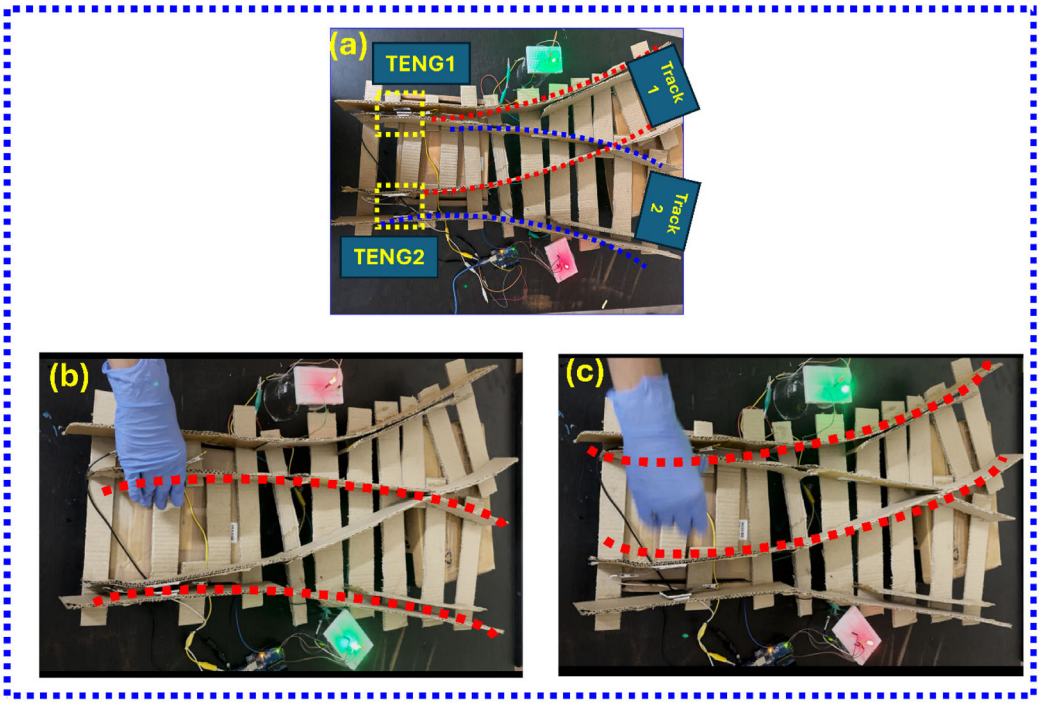

FIGURE 5 | (a) Model track design, (b,c) active railway tracks highlighted with red dots enabled by TENG sensors. TENG = triboelectric nanogenerator technology.

the driver which track is active. To monitor railway switch movements, two TENGs act as sensing elements in the design. Two TENG devices were strategically placed at the switch points of model tracks, highlighted in yellow square boxes. The electrical signals generated by the TENGs were interfaced with an Arduino board, which controlled two LED indicators, one green and one red for each track side, providing visual feedback on the switch status. The TENGs were positioned to detect mechanical movements of the switch rails, simulated by hand push force, mimicking the action of a railway switch or train load. The system provides accurate and reliable indication of track status, critical for railway operations. When the switch moves correctly, one TENG is activated and the other released, resulting in a green light for the active track and a red light for the inactive track.

The real-time demonstration of the above process is presented in Video S7, supporting information.

When the switch aligns with a track (e.g., Track 2), the corresponding TENG (TENG 2) is compressed, generating a voltage signal, while the other TENG (TENG 1) on the opposite side (Track 1) is released, producing a voltage signal. The Arduino processes these signals to activate a green LED for the aligned track (e.g., Track 2) to indicate it is active and a red LED for the unaligned track (Track 1) to mark it as inactive. In Figure 5b,c, a red LED indicates an inactive track, while a green LED indicates an active track. Conversely, when the switch aligns with another track (e.g., Track 1), Track 1 is active, and Track 2 is inactive, with green and red LED indicators. This setup ensures real-time feedback, as the TENGs respond instantly to mechanical changes, updating the LED indicators accordingly. The TENG demonstrates the fast response (<30 ms), excellent repeatability, and negligible false triggering, confirming the reliability of the proposed self-powered rail-switch sensing system. The self-powered nature of TENG sensors makes this system particularly suitable for remote railway locations, where power supply may be limited. At the same time, the real-time response ensures timely updates, avoiding delays that could lead to miscommunication in high-speed or busy rail networks.

4 | Conclusions

In this work, we have upcycled expired SS waste for energy harvesting using TENG technology and utilized it for sensor applications. The SS-FEP TENG exhibited a power density of 5.7 W/m^2 and were capable of powering 240 LEDs. The self-powered sensor in rail switch systems provided real-time, reliable track status indications, enhancing rail safety and operational efficiency. By transforming nonbiodegradable waste into a valuable energy resource, this work addresses critical environmental challenges, aligning with SDGs such as responsible consumption and production. This research paves the way for the broader adoption of TENGs as new WTE technologies for a sustainable future and self-powered sensing.

Author Contributions

Anusha Kaki: data curation, formal analysis, investigation, methodology, validation, visualization, writing – original draft, and writing – review & editing. **Mahesh Velpula**: data curation, formal analysis, investigation, software, validation, and writing – review & editing. **Navaneeth Madathil**: data curation, formal analysis, software, validation, and writing – review & editing. **Khanapuram Uday Kumar**: formal analysis, project administration, validation, and writing – review & editing. **Ravinder Reddy Kisannagar**: software, validation, and writing – review & editing. **Inhwa Jung**: formal analysis and writing – review & editing. **Rakesh Kumar Rajaboina**: conceptualization, formal analysis, methodology, project administration, supervision, writing – original draft, and writing – review & editing.

Acknowledgments

R.R.K. and K.U.K. thank the Director, National Institute of Technology, Warangal, for his constant encouragement and support in infrastructure. R.R.K. and K.U.K. acknowledge DAE-BRNS (59/14/06/2024-BRNS/717) for surface potential measurement system (electrostatic voltmeter).

Funding

This study was supported by Board of Research in Nuclear Sciences (59/14/06/2024-BRNS/717).

Conflicts of Interest

The authors declare no conflicts of interest.

Data Availability Statement

The data supporting the findings of this study are available within the article and supplementary information.

References

1. M. A. Hannan, M. A. Al Mamun, A. Hussain, H. Basri, and R. A. Begum, "A Review on Technologies and Their usage in Solid Waste Monitoring and Management Systems: Issues and Challenges," *Waste Management* 43 (2015): 509–523, https://doi.org/10.1016/J.WASMAN.2015.05.033.

2. D. Kannan, S. Khademolqorani, N. Janatyan, and S. Alavi, "Smart Waste Management 4.0: The Transition from a Systematic Review to an Integrated Framework," *Waste Management* 174 (2024): 1–14, https://doi.org/10.1016/J.WASMAN.2023.08.041.

3. https://sdgsunorg/goals, Department of Economic and Social Affairs Sustainable Development THE 17 GOALS, n.d., https://sdgs.un.org/goals-https://sdgs.un.org/goals.

4. M. W. Kleespies and P. W. Dierkes, "The Importance of the Sustainable Development Goals to Students of Environmental and Sustainability Studies—a Global Survey in 41 countries," *Humanities and Social Sciences Communications* 9 (2022): 218, https://doi.org/10.1057/s41599-022-01242-0.

5. W. Foster, U. Azimov, P. Gauthier-Maradei, et al., "Waste-to-Energy Conversion Technologies in the UK: Processes and Barriers – A Review," *Renewable and Sustainable Energy Reviews* 135 (2021): 110226, https://doi.org/10.1016/j.rser.2020.110226.

6. H. D. Beyene, A. A. Werkneh, and T. G. Ambaye, "Current Updates on Waste to Energy (WtE) Technologies: A Review," *Renewable Energy Focus* 24 (2018): 1–11, https://doi.org/10.1016/J.REF.2017.11.001.

7. R. Kothari, V. V. Tyagi, and A. Pathak, "Waste-to-Energy: A Way from Renewable Energy Sources to Sustainable Development," *Renewable and Sustainable Energy Reviews* 14 (2010): 3164–3170, https://doi.org/10.1016/J.RSER.2010.05.005.

8. P. Lisbona, S. Pascual, and V. Pérez, "Waste to Energy: Trends and Perspectives," *Chemical Engineering Journal Advances* 14 (2023): 100494, https://doi.org/10.1016/J.CEJA.2023.100494.

9. S. Armenise, W. SyieLuing, J. M. Ramírez-Velásquez, et al., "Plastic Waste Recycling via Pyrolysis: A Bibliometric Survey and Literature Review," *Journal of Analytical and Applied Pyrolysis* 158 (2021): 105265, https://doi.org/10.1016/j.jaap.2021.105265.

10. D. Cudjoe and H. Wang, "Plasma Gasification versus Incineration of Plastic Waste: Energy, Economic and Environmental Analysis," *Fuel Processing Technology* 237 (2022): 107470, https://doi.org/10.1016/j.fuproc.2022.107470.

11. L. Makarichi, W. Jutidamrongphan, and K. Techato, "The Evolution of Waste-to-Energy Incineration: A Review," *Renewable and Sustainable Energy Reviews* 91 (2018): 812–821, https://doi.org/10.1016/j.rser.2018.04.088.

12. K. U. Kumar, S. Hajra, G. M. Rani, et al., "Revolutionizing Waste-to-Energy: Harnessing the Power of Triboelectric Nanogenerators," *Advanced Composites and Hybrid Materials* 7 (2024): 91, https://doi.org/10.1007/s42114-024-00903-9.

13. Y. Wang, Z. Li, H. Fu, and B. Xu, "Sustainable Triboelectric Nanogenerators Based on Recycled Materials for Biomechanical Energy Harvesting and Self-Powered Sensing," *Nano Energy* 115 (2023): 108717, https://doi.org/10.1016/J.NANOEN.2023.108717.

14. S. Chao, H. Ouyang, D. Jiang, Y. Fan, and Z. Li, "Triboelectric Nanogenerator Based on Degradable Materials," *EcoMat* 3 (2021): 1–19, https://doi.org/10.1002/eom2.12072.

15. S. A. Basith, G. Khandelwal, D. M. Mulvihill, and A. Chandrasekhar, "Upcycling of Waste Materials for the Development of Triboelectric Nanogenerators and Self-Powered Applications," *Advanced Functional Materials* 34 (2024): 2408708, https://doi.org/10.1002/adfm.202408708.

16. P. R. Sankar, P. Supraja, S. Mishra, K. Prakash, R. R. Kumar, and D. Haranath, "A Novel Triboelectric Nanogenerator Based on Only Food Packaging Aluminium Foils," *Materials Letters* 310 (2022): 131474, https://doi.org/10.1016/j.matlet.2021.131474.

17. X. Feng, Q. Li, and K. Wang, "Waste Plastic Triboelectric Nanogenerators Using Recycled Plastic Bags for Power Generation," *ACS Applied Materials & Interfaces* 13 (2021): 400–410, https://doi.org/10.1021/acsami.0c16489.

18. F. Ali, Z. Hussain, M. Numan, et al., "Triboelectric Nanogenerator Based on PTFE Plastic Waste Bottle and Aluminum Foil," *Materials Innovations* 2 (2022): 203–213, https://doi.org/10.54738/mi.2022.2803.

19. G. Han, B. Wu, and Y. Pu, "A Triboelectric Nanogenerator Based on Waste Plastic Bags for Flexible Vertical Interconnection System," *Microsystem Technologies* 26 (2020): 3893–3899, https://doi.org/10.1007/s00542-020-04879-6.

20. M. Navaneeth, S. Potu, A. Babu, et al., "Transforming Medical Plastic Waste into High-Performance Triboelectric Nanogenerators for Sustainable Energy, Health Monitoring, and Sensing Applications," *ACS Sustainable Chemistry & Engineering* 11 (2023): 12145–12154, https://doi.org/10.1021/acssuschemeng.3c03136.

21. M. Navaneeth, S. Potu, A. Babu, et al., "A Medical Waste X-Ray Film Based Triboelectric Nanogenerator for Self-Powered Devices, Sensors, and Smart Buildings," *Environmental Science: Advances* 2 (2023): 848–860, https://doi.org/10.1039/D3VA00018D.

22. S. A. Basith and A. Chandrasekhar, "COVID-19 Clinical Waste Reuse: A Triboelectric Touch Sensor for IoT-Cloud Supported Smart Hand Sanitizer Dispenser," *Nano Energy* 108 (2023): 108183, https://doi.org/10.1016/j.nanoen.2023.108183.

23. X. Liang, Z. Liu, K. Han, et al., "Triboelectric Nanogenerators Using Recycled Disposable Medical Masks for Water Wave Energy Harvesting," *Advanced Functional Materials* 34 (2024): 2409422, https://doi.org/10.1002/ADFM.202409422.

24. V. L. Sunitha, P. Supraja, K. A. K. D. Prasad, et al., "Wood Plastic Composites (WPC) Waste Based Triboelectric Nanogenerator for Mechanical Energy Harvesting and Self-Powered Applications," *Materials Letters* 351 (2023): 134995, https://doi.org/10.1016/J.MATLET.2023.134995.

25. A. Kaki, G. Maharana, N. Madathil, et al., "Electronic Waste to Energy: Self-Powered Electronic Devices and Organic Dye Degradation Using TENG-Assisted Photocatalysis," *Advanced Sustainable Systems* 9 (2025): e00235, https://doi.org/10.1002/ADSU.202500235, WGROUP:STRING: PUBLICATION.

26. M. U. Bukhari, A. Khan, K. Q. Maqbool, A. Arshad, K. Riaz, and A. Bermak, "Waste to Energy: Facile, Low-Cost and Environment-Friendly Triboelectric Nanogenerators Using Recycled Plastic and Electronic Wastes for Self-Powered Portable Electronics," *Energy Reports* 8 (2022): 1687–1695, https://doi.org/10.1016/j.egyr.2021.12.072.

27. C. S. Patil, Q. M. Saqib, S. R. Patil, et al., "Triboelectric Nanogenerator Based on Reactivated Electrode Materials Derived from Waste Alkaline Battery: Influence of Pyrolysis Temperature and Surface Morphology," *Nano Energy* 121 (2024): 109205, https://doi.org/10.1016/j.nanoen.2023.109205.

28. R. F. S. M. Ahmed, S. Amini, S. M. Ankanathappa, and K. Sannathammegowda, "Electricity Out of Electronic Trash: Triboelectric Nanogenerators from Discarded Smartphone Displays for Biomechanical Energy Harvesting," *Waste Management* 178 (2024): 1–11, https://doi.org/10.1016/j.wasman.2024.02.009.

29. V. L. Suneetha, V. Mahesh, P. Supraja, M. Navaneeth, K. U. Kumar, and R. R. Kumar, "Facile and Robust High-Performance Triboelectric Nanogenerator Based on Electronic Waste for Self-Powered Electronics," *Energy Technology* 13 (2025): 2401387, https://doi.org/10.1002/ente.202401387.

30. B. M. Sankarshan, M. D. P. Girigowda, S. M. R. Farheen, et al., "E-Waste Resistors-Based Triboelectric Nanogenerators for Sustainable Energy Harvesting and Self-Powered Electronics," *Sensors and Actuators A: Physical* 394 (2025): 116918, https://doi.org/10.1016/J.SNA.2025.116918.

31. L. S. Vikram, S. Potu, D. P. Kasireddi A. K., U. K. Khanapuram, H. Divi, and R. K. Rajaboina, "Biowaste Sea Shells-Based Triboelectric Nanogenerator: Sustainable Approach for Efficient Mechanical Energy Harvesting," *Energy Technology* 13 (2025): 2401333, https://doi.org/10.1002/ente.202401333.

32. A. Gaur, S. Tiwari, C. Kumar, and P. Maiti, "Bio-Waste Orange Peel and Polymer Hybrid for Efficient Energy Harvesting," *Energy Reports* 6 (2020): 490–496, https://doi.org/10.1016/j.egyr.2020.02.020.

33. R. A. Shaukat, Q. M. Saqib, M. U. Khan, M. Y. Chougale, and J. Bae, "Bio-Waste Sunflower Husks Powder Based Recycled Triboelectric Nanogenerator for Energy Harvesting," *Energy Reports* 7 (2021): 724–731, https://doi.org/10.1016/j.egyr.2021.01.036.

34. S. Xu, P. Huang, Y. Luo, et al., "High Value-Added Development of Waste Cellulose Peels for Bio-Piezoelectric Membrane in Nanogenerator-Derived Self-Powered Sensor," *Journal of Materials Science: Materials in Electronics* 34 (2023): 1414, https://doi.org/10.1007/s10854-023-10844-6.

35. M. Tiwari and D. Bharti, "Biowaste-Based Triboelectric Nanogenerators Using Peanut Skin for Energy Harvesting and Real-Time Sensing," *Sustainable Materials and Technologies* 45 (2025): e01472, https://doi.org/10.1016/J.SUSMAT.2025.E01472.

36. S. Panda, H. Song, S. Hajra, et al., "Detection of Biogenic Amine Histamine Using a Triboelectric Nanogenerator Integrated Biodegradable Sensor," *Journal of Materials Chemistry B* 13 (2025): 13272–13281, https://doi.org/10.1039/D5TB01337B.

37. G. M. Rani, S. M. Ghoreishian, R. Umapathi, V. Vivekananthan, and Y. S. Huh, "A Biocompatible Triboelectric Nanogenerator-Based Edible Electronic Skin for Morse Code Transmitters and Smart Healthcare Applications," *Nano Energy* 128 (2024): 109899, https://doi.org/10.1016/J.NANOEN.2024.109899.

38. R. Vamsi, D. K. Harshitha, K. Manojkumar, et al., "Unraveling the Energy-Harvesting Performance of Antimony-Doped BaTiO3 Toward Self-Powered on-Body Wearable Impact Sensor," *Energy Technology* 13 (2025): 2500047, https://doi.org/10.1002/ENTE.202500047.

39. S. Hajra, S. Panda, K. R. Kaja, M. A. Belal, V. Vivekananthan, and H. J. Kim, "Self-Powered Fire Safety Indicator Based on Fabric-Based Triboelectric Nanogenerator," *Energy Technology* 13 (2025): 2402488, https://doi.org/10.1002/ENTE.202402488.

40. A. A. Mathew, A. Chandrasekhar, and S. Vivekanandan, "A Review on Real-Time Implantable and Wearable Health Monitoring Sensors Based on Triboelectric Nanogenerator Approach," *Nano Energy* 80 (2021): 105566, https://doi.org/10.1016/j.nanoen.2020.105566.

41. P. Munirathinam and A. Chandrasekhar, "Wearable Triboelectric Nanogenerator for Real-Time IoT-Supported Security Applications," *Sustainable Materials and Technologies* 37 (2023): e00700, https://doi.org/10.1016/j.susmat.2023.e00700.

42. K. L. Mittal and A. Pizzi, 2009, *Handbook of Sealant Technology*, 1st ed., CRC Press, CRC, accessed June 11, 2025, https://www.routledge.com/Handbook-of-Sealant-Technology/.

43. S. Radhakrishnan, S. Joseph, E. J. Jelmy, K. J. Saji, T. Sanathanakrishnan, and H. John, "Triboelectric Nanogenerators for Marine Energy Harvesting and Sensing Applications," *Results in Engineering* 15 (2022): 100487, https://doi.org/10.1016/J.RINENG.2022.100487.

44. S. Kumar, R. K. Jha, P. Sharma, and A. Goswami, "Design and Development of a Horizontal Contact Separated (HCS) Test Setup for Measuring the Performance of Triboelectric Nanogenerator for Sustainable Energy Harvesting Applications," *Review of Scientific Instruments* 95 (2024): 035002, https://doi.org/10.1063/5.0190787.

45. J. Bird, *Electrical Circuit Theory and Technology, Electrical Circuit Theory and Technology*, (2nd ed.) (2003), https://doi.org/10.4324/9780080505169.

Supporting Information

Additional supporting information can be found online in the Supporting Information section. **Supporting Fig. S1**: Transparent silicon sealant waste-based TENG with different frictional layers: PET (Black), silicone rubber (red), FEP (Blue) (inset: transparent expired silicone waste film on aluminum). **Supporting Video S1:** Surface potential measurements. **Supporting Video S2:** Polarity change testing. **Supporting Video S3:** Powering LEDs with hand tapping. **Supporting Video S4:** Powering four LED lamps. **Supporting Video S5:** Powering calculator with TENG. **Supporting Video S6:** Powering digital watch with TENG. **Supporting Video S7:** Demonstration rail safety type.